CHAPTER IV
RESULTS AND DISCUSSION

Precipitation of Ca – ATMP crystals in supersaturation solution was investigated. Calcium – ATMP precipitates were prepared according to the following reaction;

$$Ca^{2+} + ATMP^{2-} \rightarrow CaATMP \qquad (4.1)$$

Ca-ATMP crystals were allowed to grow at 25°C in the absence or in the presence of monovalent salt (LiCl, NaCl, and KCl) at several supersaturation ratios. The experimental results of induction time, crystal size, and composition are presented below.

This thesis was divided into two main experimental sections: nucleation and growth of Ca-ATMP precipitates. The calculation method of deprotonation and complexation of Ca-ATMP is given in Appendix B. All experimental data are shown in Appendix C.

4.1 Nucleation Kinetics

A kinetic parameter, which is measured during the nucleation, is an induction time, t_{ind}. During the induction time all chemical parameters of the system (eg. pH, concentration) remained constant which were confirmed by the withdrawal of sample and analyzed for pH and ATMP concentration by Hach technique. An example of typical turbidity curve for Ca-ATMP precipitation is shown in Figure 4.1(a). It can be seen that the turbidity was constant with time in the first 100 sec and then increased rapidly. The time that corresponds to this inflection is referred as the induction time as shown in Figure 4.1(b). It shows ΔAbs (ΔAbs = Abs at t_2 – Abs at t_1) as a function of time between t_{ind} and 250 sec (t_{ind} =125 s in this case) (Mahmoud, 2004).

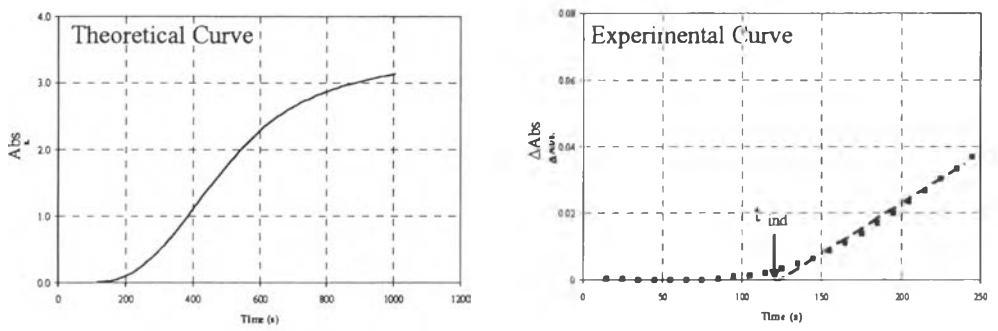

(a) (b)

Figure 4.1 (a)Typical precipitation curves (b)Enlarged turbidity–time curves showing t_{ind} for the operating conditions [ATMP] = [$CaCl_2$] = 0.05 M, pH 1.5 and temperature =25°C.

4.2 Effect of pH on Induction Time

The effect of the solution pH (pH 1.5, 4, and 7) on induction time of Ca-ATMP is shown in Figure 4.2 for different solution pH values at a fixed initial ATMP concentration of 0.04 M and a Ca/ATMP molar ratio of 1:1. The results show that the order induction period of Ca-ATMP precipitate is pH 7 < pH 1.5 < pH 4. The compositions and morphologies of Ca-ATMP precipitates are shown in Table 4.1 and Figure 4.3, respectively. The results are in good agreement with the previous study (Rarkpattanapipat, 1996) which showed that the formation of precipitates strongly depended on solution pH and the precipitates had Ca/ATMP molar ratios of 1, 2 and 3 at pH values of 1.5, 4 and 7, respectively. However, in this work, the $CaCl_2$/ATMP ratio was kept constant at 1, therefore the molar product of [Ca][ATMP] is too low to obtain a Ca/ATMP precipitate with a molar ratio of 2 at pH 4.

At pH 7, the induction time is much faster than those at pH 1.5 and 4. The difference in Ca/ATMP molar ratios results in the different induction times. The precipitate having a Ca/ATMP molar ratio of 3 can precipitate out much faster than that having a Ca/ATMP molar ratio of 1. The induction time at pH 1.5 is faster than

that at pH 4 because the initial free calcium concentration in the solution at pH 1.5 (0.0383 M) is higher than that at pH 4 (0.021 M). Therefore, at pH4 calcium is the limiting reactant for this reaction as compared to that at pH

1.5. This work focuses on induction and precipitation at pH 1.5 because we are primarily interested in only a 1:1 Ca/ATMP precipitated.

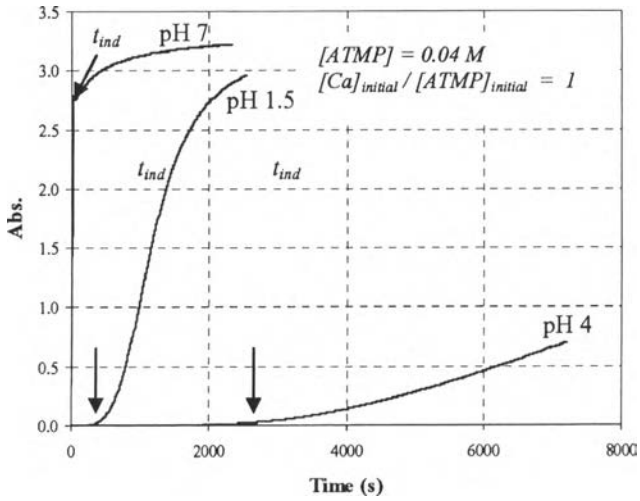

Figure 4.2 The effect of solution pH on induction time of Ca-ATMP precipitates.

Table 4.1 The dependence of compositions of Ca-ATMP precipitates on different solution pHvalues (initial ATMP concentration = 0.04M and initial malar ratio of Ca / ATMP = 1).

pH	Ca/ATMP molar ratio
1.5	1.00
4.0	1.02
7.0	3.00

(a) (b) (c)

Figure 4.3 The morphology of Ca-ATMP precipitates at different pHs: (a) pH 1.5, Ca/ATMP molar ratio = 1, (b) pH 4.0, Ca/ATMP molar ratio = 1and (c) pH 7.0, Ca/ATMP molar ratio = 3.

4.3 Effect of Monovalent Salt (LiCl, NaCl, and KCl) on Induction Time at Different Concentrations

Effect of the addition of monovalent salt in the concentration range of 0 to 0.10 M on Ca-ATMP precipitate was studied. An example of the effect of NaCl concentration at $[ATMP]_{initial}$ = 0.049M is given in Figure 4.4. It is clear that NaCl inhibits the crystallization of Ca-ATMP as indicated by longer induction times. In

cases of LiCl and KCl, they also inhibit the crystallization as shown in Figure 4.5. The order of inhibition in terms of induction time is LiCl < NaCl < KCl.

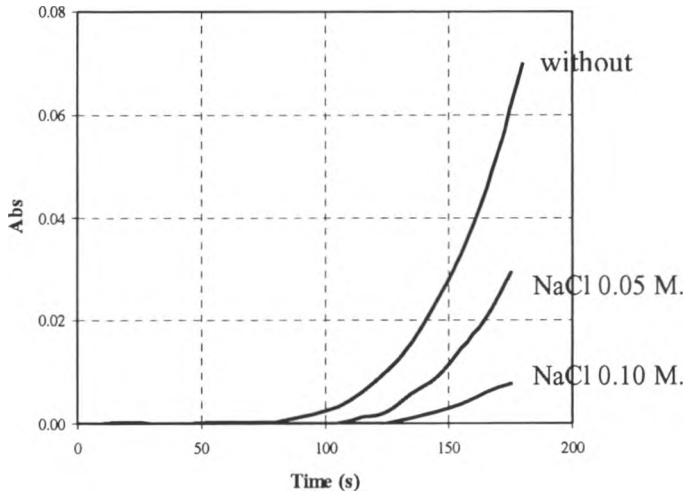

Figure 4.4 Effect of NaCl concentration on induction time at condition [ATMP] = [$CaCl_2$] = 0.049 M and pH 1.5.

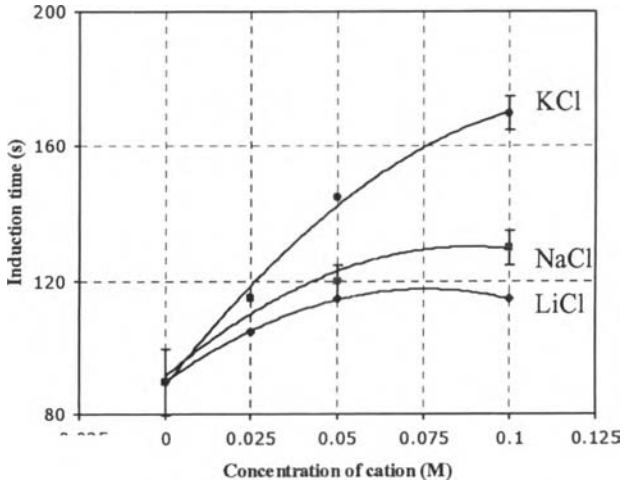

Figure 4.5 Effect of LiCl, NaCl, and KCl concentration on induction time at [ATMP] = [$CaCl_2$] = 0.0488 M and pH 1.5.

4.4 Effect of Initial ATMP Concentration on Induction Time with and without Monovalent Salt

Induction times were determined at different initial ATMP concentrations with and without monovalent salts. Figure 4.6 shows the induction times obtained from experiments using various initial reagent concentrations of ATMP without monovalent salt. The results showed that the induction time of Ca-ATMP precipitate decreased exponentially as the initial ATMP concentrations increased at a constant temperature. The results showed the same trend where a monovalent salt was present. These results also confirm that LiCl, NaCl, and KCl consistently delay Ca-ATMP nucleation as the induction time is longer as compared to that in the absence of salt. The order of nucleation inhibition is LiCl < NaCl < KCl.

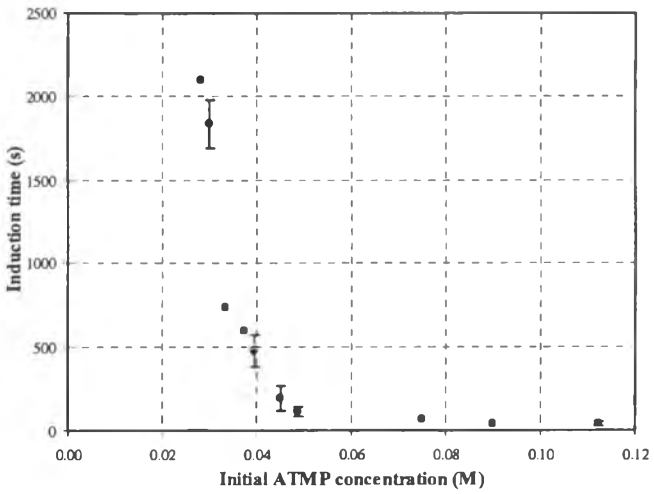

Figure 4.6 Induction time as a function of initial concentration of ATMP and initial [ATMP]/[$CaCl_2$] = 1.

4.5 Relationship between Supersaturation Ratio and Induction Time

The relation between $\ln(t_{ind})$ and $1/\ln^2(S)$ with and without 0.05M LiCl, NaCl, and KCl for Ca-ATMP precipitation at pH 1.5 is shown in Figure 4.7. One can

see that the dependence is approximately linear at high supersaturation ratios, but a few of the points at low supersaturation ratios do not fall on this straight line. This result suggests that the homogeneous theory holds validity only at high supersaturation ratio. The deviation at low supersaturation ratio is attributed to the increasing probability of heterogeneous nucleation. The surface free energy values of different precipitates estimated from slope of the graph in Figure 4.7 and calculated from Eq.(2.8) are shown in Figure 4.8. It is clear that, the surface energy is increased by addition of LiCl, NaCl and KCl. An increase in surface energy leads to decreasing the nucleation rate of Ca-ATMP precipitates as seen in Eq. (2.5). The nucleation rate, free energy for formation of critical nucleus size and radius of critical nucleus of Ca-ATMP for homogeneous nucleation are shown in Table 4.2, and in Figures 4.9 and 4.10. It is clear that the nucleation rate increases with increasing supersaturation ratio with and without monovalent salt as seen in Figure 4.9.

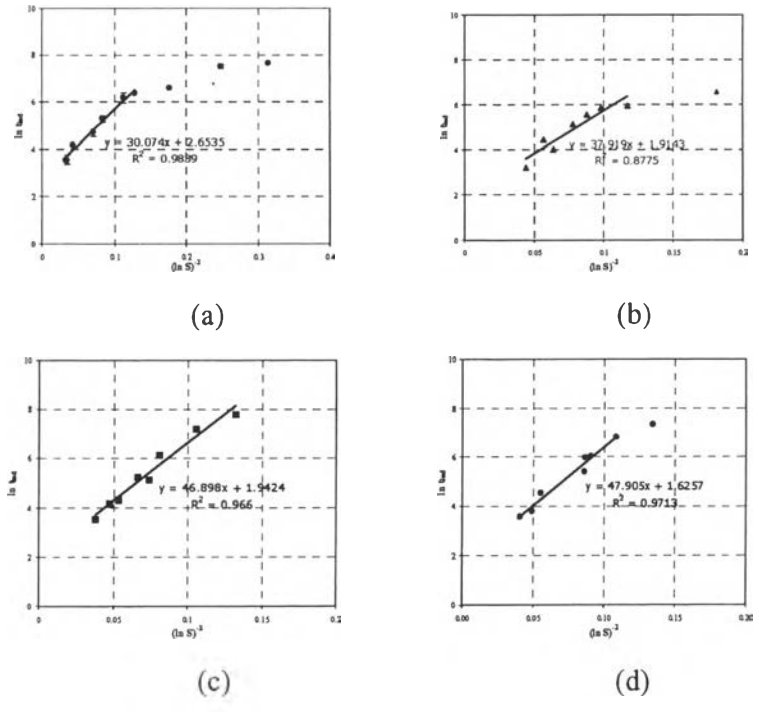

Figure 4.7 The logarithm of induction time versus $(\ln S)^{-2}$ for Ca-ATMP precipitate: (a)without salts, (b) with LiCl 0.50 M., (c)with NaCl 0.50 M. and (d) with KCl 0.50 M.

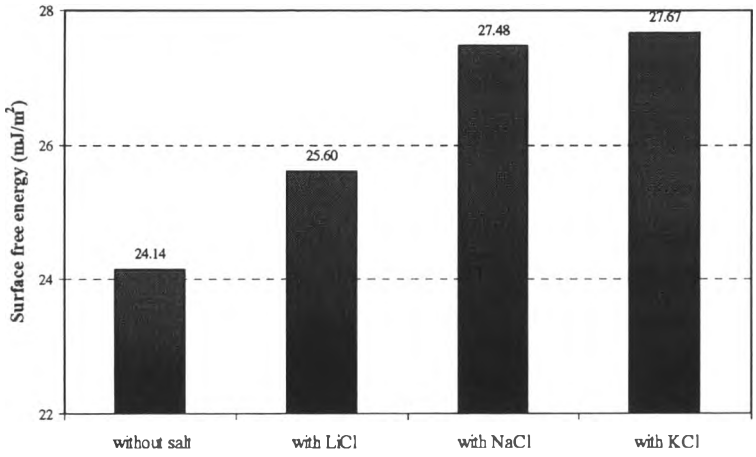

Figure 4.8 Calculated values ofsurface free energy of Ca-ATMP precipitates at pH 1.5 and 25°C with and without monovalent salt.

Moreover, addition of NaCl, LiCl, and KCl decreases the nucleation rate at all studied supersaturation ratios when compared with baseline in the absence of salts. For example, the nucleation rate at a supersaturation ratio of 6 is 5.76×10^{25} nuclei/cm^{3}s for without salt, on the other hand, the rates are 0.72×10^{25}, 0.04×10^{25}, and 0.03×10^{25} nuclei/cm^{3}s with LiCl, NaCl, and KCl, respectively.

Table 4.2 Effect of monovalent salt on nucleation rate, free energy for formation of critical nucleus of Ca-ATMP precipitates at different supersaturation ratio.

	J (*10^{28} nuclei/cm^{3}sec)				r (Å)				ΔG (*10^{-20} J)			
S	without	LiCl	NaCl	KCl	without	LiCl	NaCl	KCl	without	LiCl	NaCl	KCl
5	1.90	0.19	0.01	0.01	80.69	85.57	91.86	92.49	146.70	174.96	216.41	220.93
6	5.76	0.72	0.04	0.03	72.48	76.87	82.51	83.08	118.37	141.17	174.61	178.26
7	12.47	1.83	0.14	0.10	66.74	70.78	75.97	76.50	100.36	119.69	148.04	151.13
8	22.22	3.68	0.33	0.25	62.45	66.23	71.09	71.59	87.88	104.81	129.64	132.35
9	34.87	6.37	0.65	0.50	59.11	62.68	67.28	67.75	78.71	93.87	116.11	118.54
10	50.20	9.91	1.12	0.88	56.40	59.81	64.21	64.65	71.67	85.48	105.73	107.94

The free energy for formation of critical nucleus size decreases with increasing supersaturation ratio and increases with the addition of salt additives. The higher free energy, the more difficult precipitation occurs. The radius of the critical nucleus decreases with increasing the supersaturated ratio and with the addition of LiCl, NaCl, and KCl as shown in Figure 4.10.

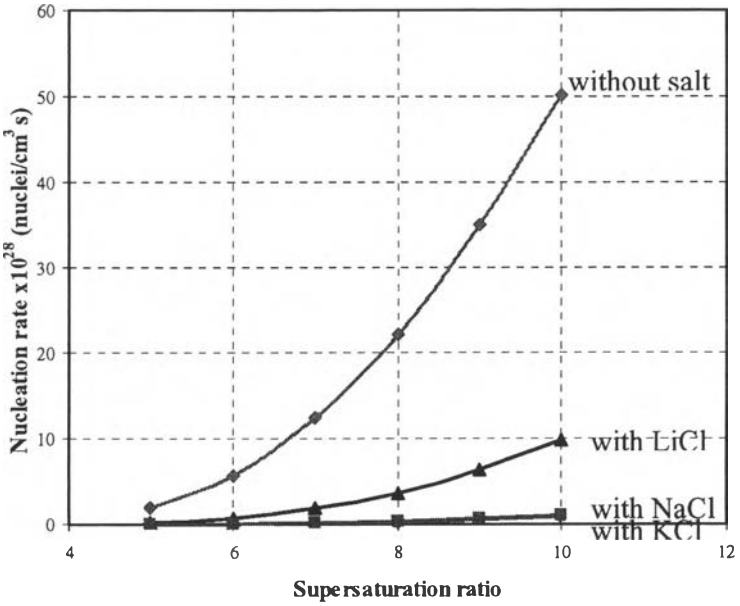

Figure 4.9 Effect of supersaturation ratio on the nucleation rate with and without monovalent salt.

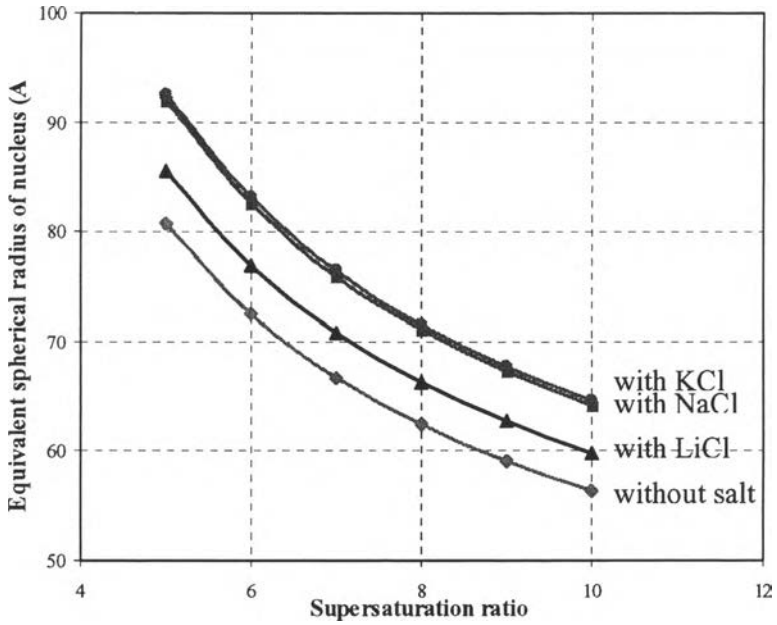

Figure 4.10 Effect of supersaturation ratio on the equivalent spherical radius of Ca-ATMP precipitates with and without monovalent salt.

4.6 Growth Kinetics

In the metastable supersaturation region, the seed crystal growth of Ca-ATMP was measured for various types of salt additives. The growth period which allows seed Ca-ATMP to grow was fixed at 20 min, the precipitation temperature was fixed at 25°C. The initial equivalent spherical radius of the seed crystals was in the range of 3.75 – 5.50 μm and the average equivalent spherical radius (L_1) was 5 μm. The supersaturation ratio was varied between 5 and 13. The supersaturated solutions had been stable before the seed was added. Figure 4.11 shows scanning electron microscopy (SEM) pictures of Ca-ATMP crystals before and after growth. It clearly confirms that no nucleation occurred because small crystals were not formed after growth.

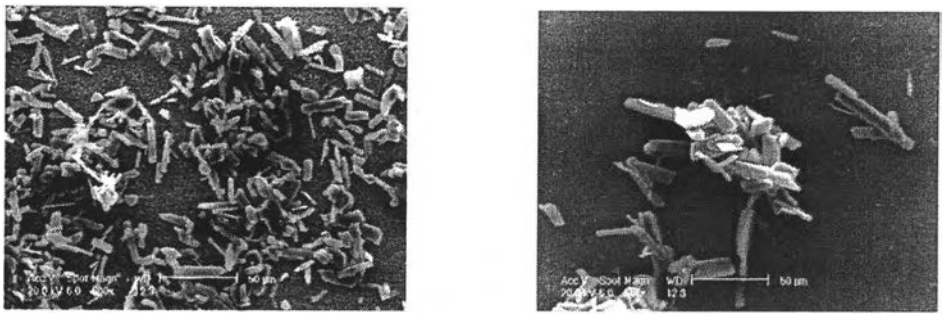

(a) (b)

Figure 4.11 Scanning electron microscopy pictures of Ca-ATMP crystals (a) before, and (b) after growth(20min).

4.7 Effect of Monovalent Salts (LiCl, NaCl, and KCl) on Growth Rate

Effect of the addition of monovalent salt on growth of Ca-ATMP precipitate was studied. An example of the effect is given in Figure 4.12 for $[ATMP]_{initial}$ = 0.075M and [salt] = 0.05 M. It is clear that growth rate of Ca-ATMP precipitate in the presence of any monovalent salt is slower than that in the absence of salt and the salt inhibits the growth of Ca-ATMP in the order of LiCl < NaCl < KCl.

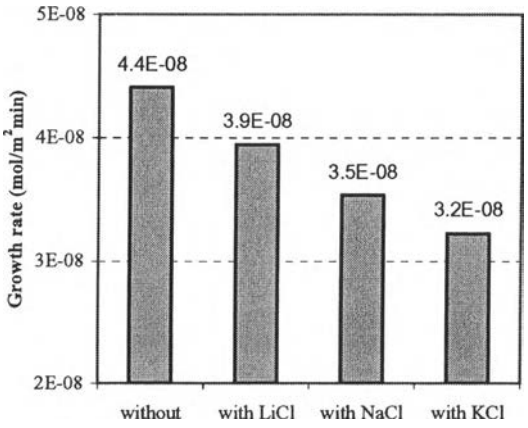

Figure 4.12 Effect of LiCl, NaCl, and KCl on Ca-ATMP growth rate at [ATMP] = $[CaCl_2]$ = 0.075 M, [salt] = 0.05M and pH 1.5.

4.8 Growth Rate Parameters

Since the total mass growth rate of the seed crystals, R, is related to the initial ATMP concentration, as expressed in Eq (2.14)

$$R_G = k_r \left[(C_b - C^*) - \frac{R_G}{k_d} \right]^r \tag{2.14}$$

The kinetic parameters of the overall equation for the crystal growth rate of Ca-ATMP precipitates were obtained from the regression using Polymath program. The kinetic parameters (k_r and r), which are independent with k_d, are displayed in Table 4.3. Therefore, the surface reaction step offers a greater resistance to the overall growth rate than the diffusion step.

Unfortunately, since no kinetic study on Ca-ATMP crystal growth has been reported, the surface reaction order measured in the current experiments could not be compared with other experimental data.

Table 4.3 The growth rate parameters

Solution	surface reaction order r	surface reaction rate constant k_r	r^2
Pure	0.93	1.00E-09	0.98
with LiCl	0.87	1.19E-09	0.98
with NaCl	0.61	3.00E-09	0.93
with KCl	1.40	1.03E-10	0.93

4.9 Growth Mechanism

In order to evaluate the microstructure of Ca-ATMP crystals, they were subjected to scanning electron microscopic (SEM) characterization. Typical SEM micrographs are shown in Figure 4.13. They show a layered growth structure of surface crystals and reveal the occurrence of layered spiral-like growth featuring

terraces that emanate from screw dislocations. Therefore, the crystal growth is soverned by a spiral growth mechanism.

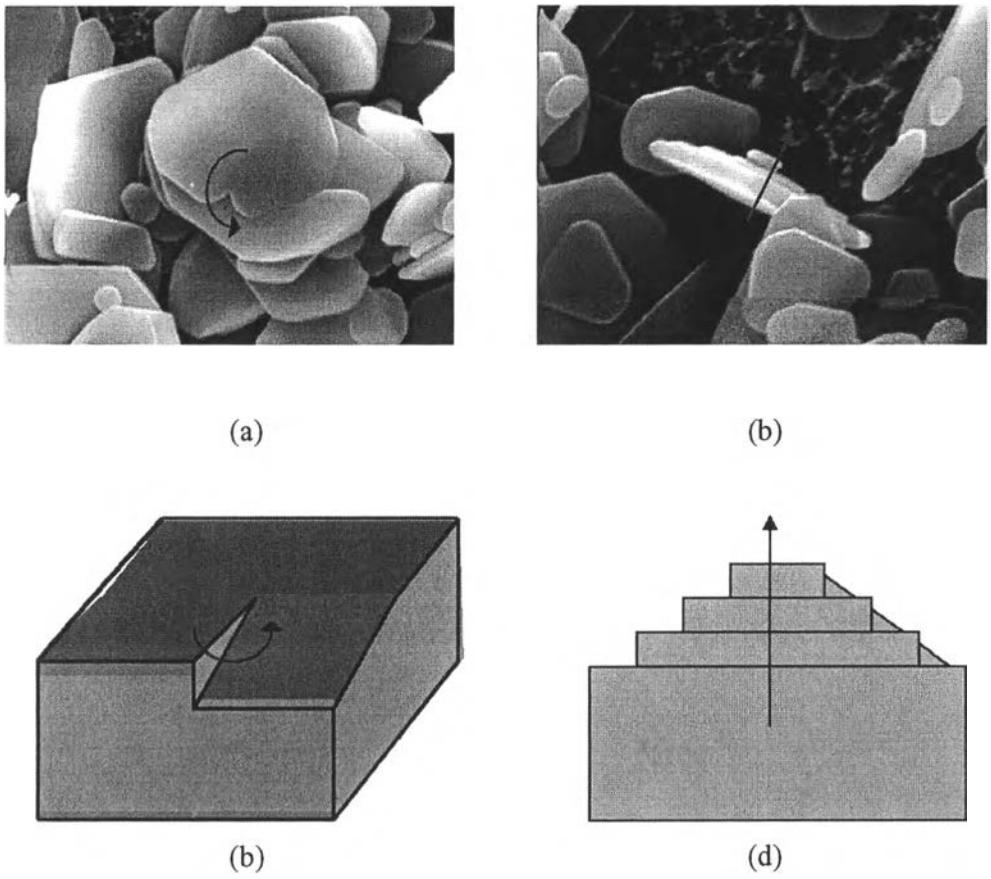

Figure 4.13 (a,b) Scanning electron microscope images(x10000) of the Ca-ATMP crystals showing spiral-like growth features and (c,d)Development of growth spiral from a screw dislocation (Mullin, 1993).

4.10 The Surface Morphology of Ca-ATMP precipitates

SEM photograph of surface morphology of Ca-ATMP precipitate is shown in Figure 4.14. As shown in SEM photographs, a lot of kinks and step terrace are visible on the Ca-ATMP crystal surface. It envisages that an apparently flat crystal

surface is in fact made up of moving layers (steps) of monoatomic height, which may contain one or more kinks. In addition, there will be loosely adsorbed growth units on crystal surface and vacancies in the surface and steps. Growth units are more easily incorporated into the crystal at a kink; the kink moves along the step and the face is eventually completed. A crystal grow faster when its face is entirely covered with kinks (Mullin, 1993).

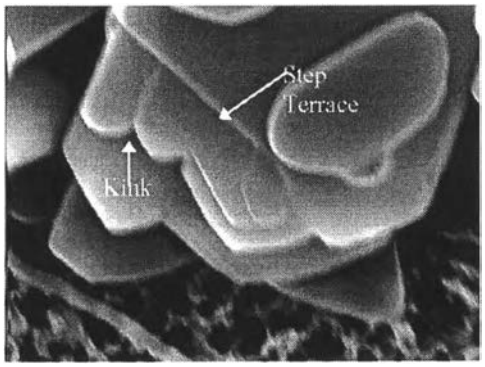

Figure 4.14 SEM photograph (x12000) of surface morphology of Ca-ATMP precipitate.